Devising tissue ingrowth metrics: a contribution to the computational characterization of engineered soft tissue healing

To cite this article before publication: Antoine Alves *et al* 2018 *Biomed. Mater.* in press https://doi.org/10.1088/1748-605X/aaa9d4

Devising tissue ingrowth metrics: a contribution to the computational characterization of engineered soft tissue healing

Antoine Alves[1&2], Nina Attik[2], Yves Bayon[3], Elodie Royet[1], Carine Wirth[1], Xavier Bourges[3], Alexis Piat[4], Gaëlle Dolmazon[1], Gaëlle Clermont[1], Jean-Pierre Boutrand[5], Brigitte Grosgogeat[2], Kerstin Gritsch[2].

[1]NAMSA France, 115 Chemin de l'Islon, 38670 Chasse-sur-Rhône, France

[2]Laboratoire des Multimatériaux et Interfaces UMR CNRS 5615, UFR Odontologie, Université Lyon 1, Université de Lyon, 69008 Lyon, France

[3]Medtronic – Sofradim Production, 116 Avenue du Formans, 01600 Trévoux, France

[4]INSA, Département Biosciences, Bâtiment Louis Pasteur11, avenue Jean Capelle, 69621 Villeurbanne cedex

[5]NAMSA 6750 Wales Road, Northwood, Ohio 43619, USA

Abstract

The paradigm shift brought about by the expansion of tissue engineering and regenerative medicine away from the use of biomaterials, currently questions the value of histopathologic methods in the evaluation of biological changes. To date, the available tools of evaluation are not fully consistent and satisfactory for these advanced therapies. We have developed a new, simple and inexpensive quantitative digital approach that provides key metrics for structural and compositional characterization of the regenerated tissues. For example, metrics provide the tissue ingrowth rate (TIR) which integrates two separate indicators; the cell ingrowth rate (CIR) and the total collagen content (TCC) as featured in the equation, TIR%=CIR%+TCC%. Moreover a subset of quantitative indicators describing the directional organization of the collagen (relating structure and mechanical function of tissues), the ratio of collagen I to collagen III and the optical anisotropy property of the collagen (maturity indicator) was automatically assessed as well. Using an image analyzer, all metrics were extracted from only two serial sections stained with either Feulgen & Rossenbeck (cell specific) or Picrosirius Red F3BA (collagen specific). To validate this new procedure, 3D scaffolds were intraperitoneally implanted in healthy and in diabetic rats. It was hypothesized that quantitatively; the healing tissue would be significantly delayed and of poor quality in diabetic rats in comparison to healthy rats. In addition, a chemically modified 3D scaffold was similarly implanted in a third group of healthy rats with the assumption that modulation of the ingrown tissue would be quantitatively present in comparison to the 3D scaffold-healthy group. After 21 days of implantation, both hypotheses were verified by use of this novel computerized approach. When the two methods were run in parallel, the quantitative results revealed fine details and differences not detected by the semi-quantitative assessment, demonstrating the importance of quantitative analysis in the performance evaluation of soft tissue healing. This automated and supervised method reduced operator dependency and proved to be simple, sensitive, cost-effective and time-effective. It supports objective therapeutic comparisons and helps to elucidate regeneration and the dynamics of a functional tissue.

Keywords: Tissue ingrowth, Regeneration, Scaffold, Tissue engineering, Collagen, Diabetes, Quantitative pathology

AUTHOR SUBMITTED MANUSCRIPT - BMM-101971 Page 2 of 20

Introduction

As early as the mid-'50s, Sewell *et al* (1955) introduced a groundbreaking histopathologic method for evaluation of biomaterial effects that was based on a grading scale of the local tissue reaction [1]. Their contribution, aimed at reducing biases as much as possible, was linked to the evaluation of biomaterial tissue reaction that was formerly only based on subjective qualitative analysis. The Sewell systematic semi-quantitative method with a Tissue Reactivity Score now allows for a pertinent comparison of biomaterial local effects [2]. Continuous improvements from use of this systematic analytic method were even found in international standards (e.g. ASTM F981-93 recommends using the Histopathologic Toxicity Rating and more recently (2007), the Irritant Ranking Score appears in ISO 10993-6 (2016) that evolved into the Reactivity Ranking Score [3].

International standards helped in guiding developers evaluate the biological risk associated with new therapeutic products, but some limitations might occur. For instance, international standards recommend using a comparative semi-quantitative microscopic evaluation to determine the local tissue effects of new implants compared to reference devices with equivalent clinical indications. The evaluation of local tissue effects, according to current standard is primarily based on local tolerance parameters, which may insufficiently assess the efficacy of the treatment, in some cases such as the restoration or regeneration of defective soft tissues. Semi-quantitative score-based assessment still remains subjective as it mostly depends on the experience and interpretation of the readers. This is particularly stressed when implant performance matters for its intended functions [4]. Statistical quantitative analysis is then desired for unbiased and objective evaluation of innovative therapeutic products whether for screening or as a last step testing.

With bone tissue evaluation, there are many available and commonly used investigative tools (e.g. radiography, quantitative computed tomography and microCT, magnetic resonance imaging, single-photon absorptiometry, faxitron, SEM, histomorphometry and more to characterize the bone healing stage [5–10]. For soft tissue therapies, quantitative methods are not routinely used for the evaluation of key parameters such as foreign body response, implant remodeling, new tissue formation, throughout the development cycle of new products [11]. In experimental studies, among the various approaches used to determine the healing stage of tissue repair, microscopic investigations remains as the preferred method [12]. It can furnish very concise morphologic details of cellular infiltrates, features of newly formed extracellular matrix, pattern and extent of the neovascularization and innervation, biomaterial remodeling, and even biofunctionality insights. For instance, presence of bone perforating Sharpey's fibers may ascertain formation of a (resistant) biofunctional anchor of regenerated ligaments (periodontal, cranium, spine, long bone). While these detailed biologic features are not always observable with other imaging methods, it is still incompletely elucidated, which type of tissue reaction favors optimal reparative or regenerative tissue, and how precisely physicochemical properties of the biomaterials promote specific biological responses [13].

With the increasing development of biomimetic materials, drug eluting templates, functionalized and smart instructive biomaterials or tissue engineered products, the objective and comparative evaluation of local tissue effects becomes more challenging [14,15,16]. Effective and efficient methods providing quantitative assessment of newly formed tissues and product integration are thus essential [12,16,17]. Indeed, in-depth evaluation and objective comparison approaches are expected to reveal the

efficacy value of functional tissue regeneration strategies. The challenge is to both interrogate responses at cellular and extracellular levels (i.e. cell-tissue growth, inflammatory response…). Over the last twenty years, routine histomorphometric methodologies have been scarcely developed for evaluation of the dynamics of soft tissue ingrowth. As examples, have been presented in the literature: i) overall tissue content of an entire sample [18], ii) tissue area fraction in selected regions of interest [4,19,20], iii) operator definition of the tissue ingrowth front [21], iv) quantitative approach consisting of an automatic determination of the tissue content in a number of computer-defined concentric zones, v) quantitative evaluation of immunohistochemically detected inflammatory cells or fluorescently labeled outgrown cells at the implant sites [20,22-24]. These two last methods (iv and v) have the potential to eliminate biases of subjective evaluation, e.g. investigator related errors and suboptimal reproducibility [17,20,24]. However, all these methodologies may have limitations. For example, they may fail to provide tissue components, to comply with routine analyses, e.g. ease of use, implementation, cost-effectiveness, discrimination power at short healing intervals and performance predictability.

All those reasons previously mentioned, motivated the development of a novel and simple computer-based quantitative evaluation method (named by the authors SCAN-CT for structural and compositional computerized analysis of connective tissue) with implementation of tissue ingrowth metrics delivering simultaneous information about the cellularity and extracellular matrix features. To validate the methodology developed for those purposes and to select a relevant preclinical model, the following two hypotheses were developed and used in this study: (1) It is well known that there is a delayed wound healing in diabetics [25-27], therefore the tissue ingrowth should be significantly different in either cellular and/or extracellular matrix measured in specimens harvested from healthy versus diabetic rats (2) Tissue ingrowth modulation (i.e. differences in related sub-parameters) should be noticed following (fine) design or material changes.

The objective of this study was to validate an innovating simple and automated quantitative method for evaluation of the regenerated soft tissues, by assessing two intraperitoneal 3D scaffolds (meshes) implanted in diabetic or healthy rats.

Materials and Methods

Scaffolds

Two composite meshes sterilized by gamma-irradiation were implanted intra-peritoneally, in rats. They are made out of a three-dimensional (3D) monofilament polyester textile, which is covered with an absorbable, continuous and hydrophilic collagen-based film on one of its sides. They are indicated for the reinforcement of soft tissue where a weakness exists such as the repair of the primary abdominal wall and incisional hernias.

The composite 3D meshes of this study went into two distinct configurations, 1) Parietex™ Composite Mesh (PCO) (reference composite 3D mesh; PCO), 2) a prototype with a film made of a combination of oxidized collagen mixed with Chitosan (degree of acetylation [DA]: 50%) (chemically modified composite 3D mesh; DA50 mesh). These implants were considered as scaffolds for the purpose of this study. Both scaffolds had the same dimensions, i.e. 15 x 25 mm (textile) and 18 x 28 mm (film). The thickness of the scaffolds was 1.9 mm (textile) and 40 to 50 μm (film).

Animals

Fifteen male rats were involved in the present study (Charles River Laboratories France): 10 healthy Sprague Dawley OFA - SD (IOPS Caw), weighing 363 +/- 60 g (mean +/- SD), and 5 diabetic Zucker (ZDF / Crl-Lep fa/fa), weighing 363 +/- 18 g (mean +/- SD). The rats were individual housed in stainless steel suspended cages under laboratory conditions (humidity and temperature recorded daily). Humidity was maintained higher than 30% of relative humidity and temperature was maintained between 20 and 24°C. The artificial light cycle was controlled using an automatic timer (12 hours of light, 12 hours of dark). Standard rodent feed and water were provided *ad libitum*.
The protocol of the present study was consistent with the requirements of the European legislation for the protection of animals used for scientific purposes (Directive 2010/63/EU). It was approved by the local NAMSA Ethical Committee as NAMSA is an accredited facility registered at the French Department of Agriculture for animal housing, care and investigations.

Surgical procedure

The ten healthy rats were divided in two groups of five rats each. One group received the reference composite 3D mesh (PCO-Healthy Group, labelled PCO-HG) and the other received the chemically modified composite 3D mesh (labeled DA50-HG). The five diabetic rats composed a third group that received the same PCO mesh as the first healthy group. This diabetic group was labeled PCO-DG.
Animals in all groups received an analgesic agent and were anesthetized. A medial incision was made in the skin and extended through the peritoneum. The caecum was abraded using a scalpel blade (approximately 10 x 15mm) until the serosa was removed and petechial bleeding was observed. The caecum was then allowed to air dry for approximately 5 minutes. A 10 x 15mm surgical defect was created on the peritoneal surface of the abdominal wall just opposite to the caecum abrasion. The designated mesh material was sutured on the surgical defect created on the abdominal wall, with the antiadhesive film in contact with the caecum of each animal. The caecum was anatomically repositioned in the abdomen and the abdominal lining and skin were sutured closed using a silk thread (Silk dec.1, ETHICON). A dressing was applied on the abdomen. Additional sub-cutaneaous injections of buphrenorphine (Buprecare, AXIENCE SAS, 0.005 mg/Kg) were given at the end of the surgery and once a day for the following two days. The animals were observed daily for clinical signs and the dressing was changed as necessary.
The animals were euthanized on day 21 after surgery with a lethal intravenous injection of pentobarbital (Dolethal, VETOQUINOL, 1mL/kg) after intramuscular injection of tiletamine-zolazepam (Zoletil 100, VIRBAC, 10-25 mg/kg). The implanted sites were macroscopically observed, excised and fixed in 10% neutral buffered formalin.

Histologic preparation

After fixation in neutral formalin, the specimens were dehydrated in alcohol solutions of increasing concentration, cleared in xylene and embedded in paraffin. Four central 5 µm-thick cross sections were prepared from each site using a microtome (MICROM®, France). Each section was stained with one of the following staining: Safranin-Hematoxylin-Eosin (SHE) for inflammatory cells response assessment, Masson's Trichrome (MT) for general staining distinguishing particularly cells from surrounding connective tissue, Picrosirius red (PR) (using Sirius red F3BA, Colour Index 35780)

according to the Junqueira histochemistry staining technique [28] for specific stain of the collagen, and Feulgen & Rossenbeck (F&R) for specific cell nuclear staining [29].

Histopathologic and histomorphometric analyses

Qualitative and semi-quantitative histopathologic analysis

A qualitative and semi-quantitative histological evaluation of the local tissue effects of each scaffold was performed using a NIKON ECLIPSE 80i light microscope coupled with a digital camera DS-Fi1 NIKON. The following parameters were assessed: (1) cellularity [inflammatory cells and reconstructive cells {mesenchymal cells, fibroblasts, myofibroblasts, fibrocytes}], (2) extra-cellular matrix parameters [fibroplasia, collagen remodeling, fibrosis and neovascularization], and (3) implant performance parameters [tissue ingrowth and tissue integration]. These parameters were graded according to the following ordinal scale: (0) absent, (1) slight, (2) moderate, (3) marked, and (4) very marked (Table 1). Two independent readers conducted the semi-quantitative analysis.

Histomorphometric analysis

To quantitatively describe the ingrown tissue, the following metrics were evaluated as described below and outlined in figure 1:

1- Cell ingrowth rate (CIR)

The F&R-stained slides were used to determine the cell ingrowth rate (cellularity parameter). Located in the center of the mesh, a region of interest (ROI) of 8000µm length encompassing the scaffold was measured in each slide, using a Nikon Eclipse 80i microscope equipped with an image analyzer system (Tribvn, France, IPS version 4.06).
Formula of CIR was as follows: CIR = cell area (µm²) / ROI (µm²) x 100.

2- Total collagen content (TCC)

To determine the total collagen content percentage within the implanted scaffold, the PR-stained sections were analyzed within the same ROI and equipment as above. Formula of TCC was as follows: TCC = collagen area (µm²) / ROI (µm²) x 100

3- Tissue ingrowth rate (TIR)

The tissue ingrowth rate was defined as being an integrative equation plotting the cell ingrowth rate and the total collagen content together resulting in TIR% = CIR% + TCC%.

4- Collagen polymorphism

Under identical illumination conditions for all groups, the PR-stained sections were digitized under cross-polarization microscopy (CPM) (Nikon Eclipse 80i) equipped with an image analyzer system (Tribvn, France, IPS version 4.06). The collagen type I imparted a reddish -orange color whereas collagen type III displayed pale-green shades. The differential staining of the collagen types allowed their quantitative assessment by histomorphometry. Located in the center of the scaffold, a ROI of 3000µm length encompassing the scaffold was computerized after exclusion of the PET scaffold. Results were expressed as a ratio of collagen type I and type III surface areas. Under CPM, a section of spleen from a rabbit, rich in parenchymal reticulin (collagen type III) and collagen type I (spleen capsule) was prepared under the same conditions and used as positive control to accurately set the angle of the microscope polarizer (the analyzer filter being fixed) before measurement of the collagen types I and III surface areas [30].

AUTHOR SUBMITTED MANUSCRIPT - BMM-101971 Page 6 of 20

5- Collagen fibers directionality and anisotropy

To determine the preferential orientation of the newly formed collagen fibers, their directionality (directional orientation of the collagen fibers) was measured. For that measurement, the previous CPM digitized images issued from the PR-stained sections were used. In addition, from the same CPM digitized images, the optical anisotropy properties (birefringence) of the collagen fibers were quantified. For those two last automated measurements, a home-made modified version of the Image J's directionality plugin (Image J/Fiji 1.50) which was merged with another home-made algorithm for the determination of the collagen birefringence intensity, constituted a single macro. Four representative ROIs (200x300µm) placed on the extracellular matrix located between the yarn bundles, along the scaffold, were computerized for simultaneous collagen fibers directionality and birefringence determination. Vessels, nerves, adipocytes areas were avoided to prevent interferences on the calculations.

Collagen fibers directionality

For measurement of the collagen fibers directionality, the reference angle corresponded to the peritoneum and abdominal wall plane. The detection method used was the local gradient analysis offered by the directionality plugin. Detected angles were binned in a [-90; 90]° interval. Then, the measured values were fitted by subtracting a reference angle. The parameter "dominant direction angle" was the direction that presents the maximum "amount" value. The parameter "amount of dominant direction" corresponded to the percent of collagen following a given direction (dominant direction angle +/- deviation).

Collagen fibers anisotropy

Measurement of the optical anisotropy of the collagen fibers related to the quantification of the collagen birefringence obtained under polarized light of the PR-stained sections. The intensity of the birefringence (collagen maturity) was determined based on the grey level of the collagen fibers brightness (site anisotropy median, SAM) [31]. To avoid black background noise, only the pixels with a valor superior at 12 were accounted. To normalize tissue changes owing to the age of the animal compared to the gradual organizational changes of the newly formed collagen, birefringence measurements were carried out on the native submesothelial connective tissue (reference anisotropy median, RAM) adjacent to each treated site. By consequence, the metrics measuring the relative collagen maturity (CM) is given by the following formula:

$$CM = SAM/RAM \times 100$$

The normalized value brought by this metrics indicates the extent of the collagen matrix restoration and was quantified from an adaptation of the [31] with normalization of the results from native tissue analysis.

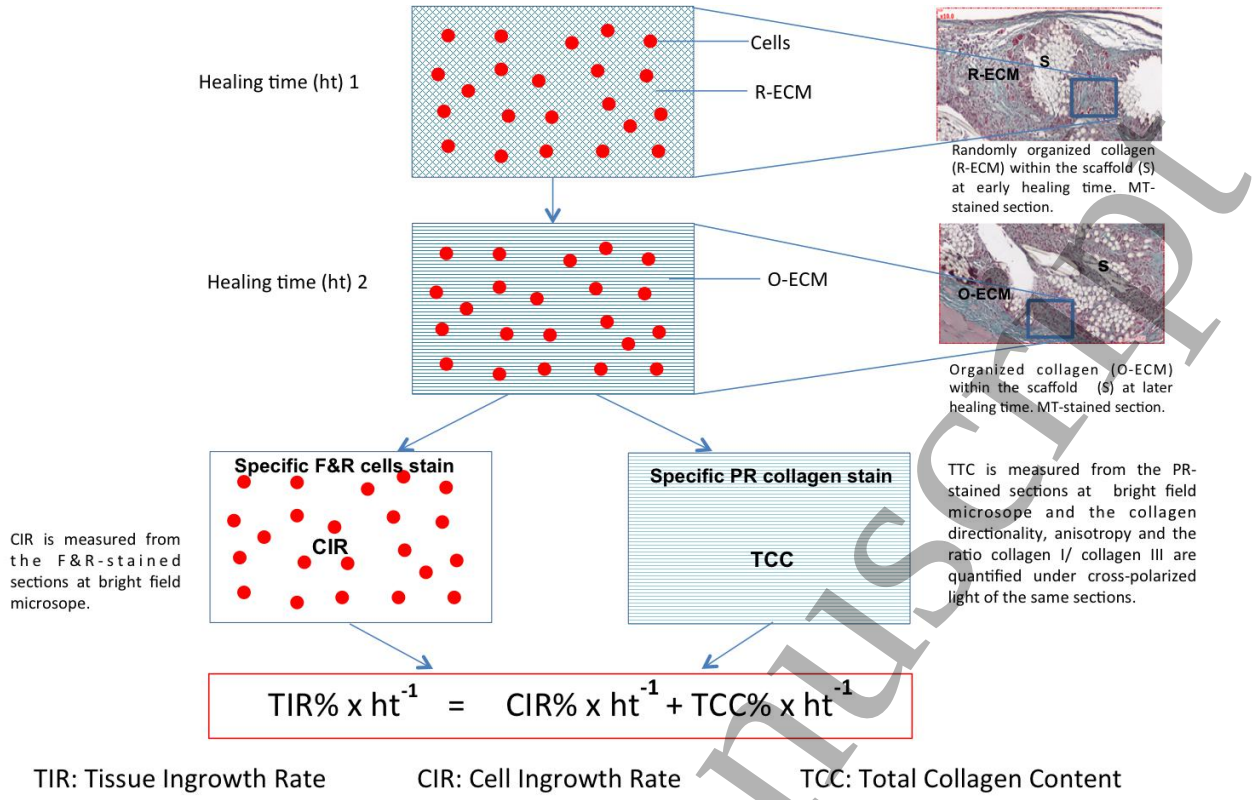

Figure 1. Schematic flow chart outlining the technical steps developed for the computerized quantitative characterization of the generated tissue. The tissue ingrowth rate is an integrative value of the cell ingrowth rate and the total amount of collagen synthetized within the scaffolds. Besides those main metrics, the collagen organization (directionality) and quality (ratio collagen I/collagen III) along with the optical anisotropy properties (collagen maturity) are provided automatically. In the TIR equation, the healing time can be simplified; still the results are provided as a function of time providing therefore a speed of tissue integration. This outline presents the methodological concept with two healing times, although in our study only one healing time was scheduled.

Statistical analysis

The results of the PCO-DG and DA50-HG were compared to that of the PCO-HG. The statistical software SPSS version 24.0, (SPSS inc.) was used to analyze the data using a Mann and Whitney test. The differences were considered to be significant at 5% critical level ($p<0.005$).

Results

Qualitative and semi-quantitative histopathologic analysis

The surgical procedure and the placement of the scaffolds were homogenous in all groups (figure 2). The antiadhesive film was practically fully degraded in all groups, 21 days, post-operatively. No evidence of intestine adhesion was observed on the sections submitted for analysis in any of the healthy animals groups. Two Zucker rats (diabetic group; DG) out of 5 showed adhesions. No signs of infection were recorded in any of the groups. No adverse effects were observed in any of the groups.

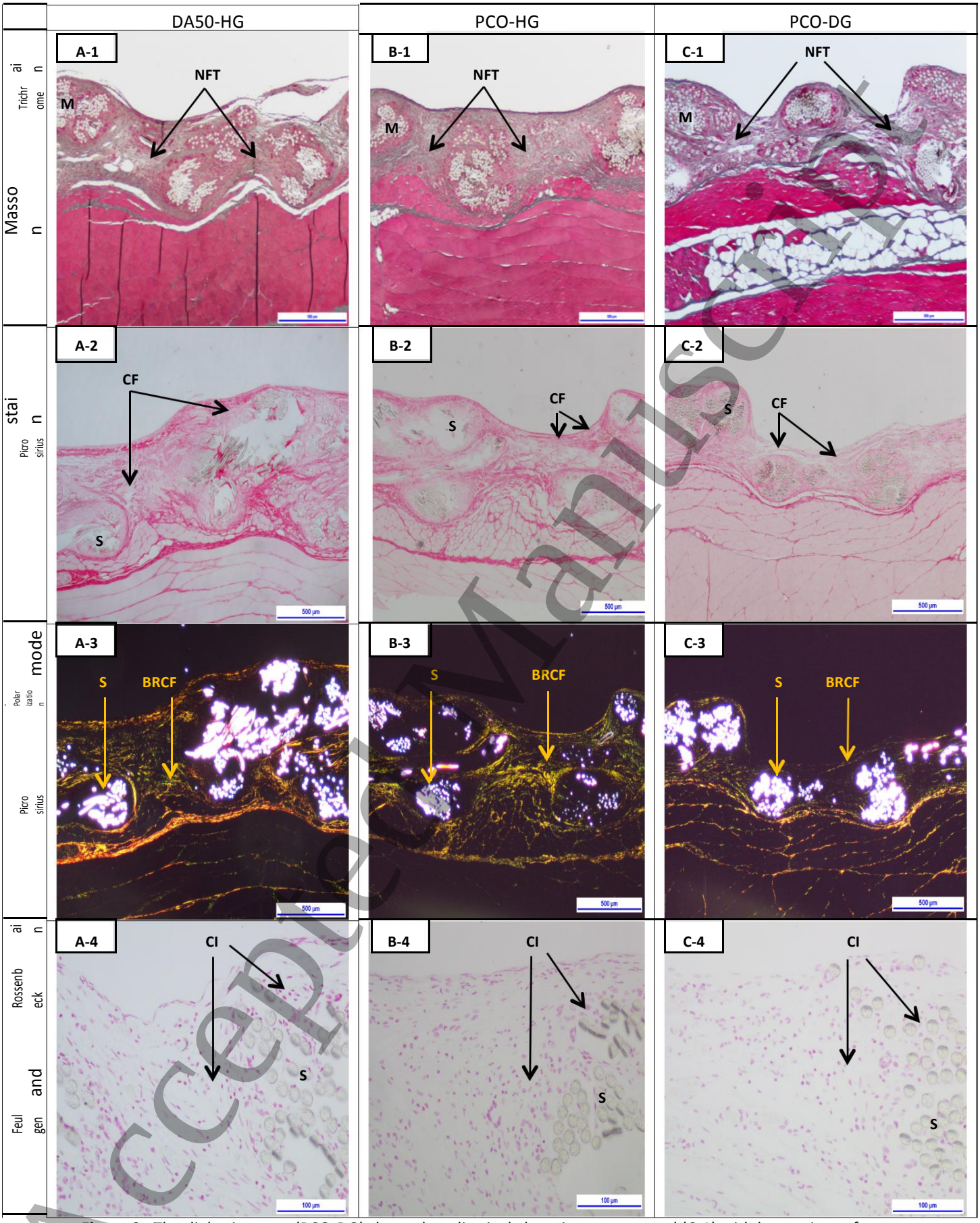

Figure 2 . The diabetic group (PCO-DG) showed qualitatively less tissue generated (C-1) with lower signs of collagen deposit (C-2, C-3) and cell ingrowth within the PCO scaffold (C-4) than the ones respectively observed

in the healthy group, either implanted with the PCO scaffold (B- 1 to B- 4) or with the chemically modified scaffold DA50-HG (A-1 to A-4). The collagen fiber directionality was similar in all groups (A-3, B-3, C-3) whereas the optical anisotropy (birefringence) was higher in DA50-HG (A-3). Abbreviation: S: Scaffold; NFT: Newly Formed Tissue; CF: Collagen Fibers, in red; BRCF: Birefringent Collagen Fibers; CI: Cell Ingrowth, in pink

The semi-quantitative analysis conducted by the two independent readers was concordant. The semi-quantitative data are summarized in table 1.

Table 1. Semi-quantitative data at 21 days (n=5/group)

	Healthy rats		**Diabetic Rats**
Parameters Mean (SD)	**PCO – HG**	**DA 50 - HG**	**PCO - DG**
Cellularity			
Reconstructive cells (mc, fb, mfb, fc)*	2.0 (0)	2.0 (0)	1.4 (0.5)
Inflammatory cells (sum of)	7.0 (0)	7.0 (0)	5.2 (1.8)
Polymorphonuclear cells	1.0 (0)	1.0 (0)	0.6 (0.5)
lymphocytes	1.0 (0)	1.0 (0)	0.6 (0.5)
plasma cells	1.0 (0)	1.0 (0)	0.6 (0.5)
macrophages	2.0 (0)	2.0 (0)	1.4 (0.5)
giant cells	2.0 (0)	2.0 (0)	2.0 (0)
Extracellular matrix parameters			
Collagen remodeling	1.0 (0)	1.0 (0)	1.0 (0)
Fibroplasia and fibrosis (sum of)	2.6 (0.5)	2.4 (0.5)	2.2 (0.4)
Fibroplasia	2.0 (0)	1.4 (0.5)	1.4 (0.5)
Fibrosis	0.6 (0.5)	1.0 (0.5)	0.8 (0.4)
Neovascularization	2.0 (0)	2.0 (0)	2.0 (0)
Implant performance parameters			
Integration	3.4 (1.2)	3.8 (0.4)	4.0 (0)
Tissue ingrowth	4.0 (0)	4.0 (0)	4.0 (0)

Grading scale: 0 absent, 1 slight, 2 moderate, 3 marked and 4 very marked

*mc : mesenchymal cells, fb : fibroblasts, mfb : myofibroblasts, fc : fibrocytes

For animals in PCO-HG, the cellularity was composed of a moderate number of reconstructive cells and inflammatory cells. The inflammatory cells were characterized by a moderate number of macrophages and multinucleated giant cells admixed with a slight number of lymphocytes, plasma cells and polymorphonuclear cells. A moderate to marked amount of collagen (fibroplasia and fibrosis) was present in the scaffold along with a slight signs of collagen remodeling. The implant performance was mainly characterized by marked tissue integration with a range from slight to marked.

The grade of cellularity (reconstructive cells and inflammatory infiltrates) in DA50-HG expression was similar to as in PCO-HG. Collagen resulting from the fibroplasia and fibrosis process was deposited at a moderate grade within the scaffold with slight signs of collagen remodeling. Slightly less signs of fibroplasia were noted than in PCO-HG. The implant performance (tissue ingrowth and integration) was not notably different compared to that of PCO-HG.

The diabetic group (PCO-DG) had a slight grade of reconstructive cells and a slight to moderate grade of inflammation cells infiltrating the scaffold. A moderate amount of collagen resulting from the

fibroplasia and fibrosis process was deposited within the scaffold with slight signs of collagen remodeling. Slightly less signs of fibroplasia were noted than in PCO-HG. The implant performance (tissue ingrowth and integration) in PCO-DG was not notably different compared to that of PCO-HG group.

In summary, there were no remarkable observational differences in the individual semi-quantitative parameters among animals in the three groups except that there was slightly less reconstructive and inflammatory cells and slightly less collagen production in the animals in the PCO-DG (table 1).

Histomorphometric analysis

The quantitative results are summarized in figure 3 and table 2. In the healthy animals (PCO-HG and DA50-HG), there were significantly fewer cells as shown by CIR values infiltrating the DA-50 scaffold compared to PCO scaffold ($p < 0.05$) (15.3 ± 3.1% vs. 22.4 ± 4.5%, respectively) (figure 3). The amount of collagen (TCC) synthetized and the resulting tissue ingrowth rate (TIR) values were not significantly different in the two healthy groups (20.5 ± 3.8% vs. 19.0 ± 2.1% for TCC, and 35.8 ± 4.7% vs. 41.4 ± 3.8% for TIR, for DA50-HG and PCO-HG, respectively).

In the diabetic group (PCO-DG), the CIR values indicated fewer cells infiltrating the scaffold with respect to the PCO-HG (17.4 ± 2.5% vs. 22.4 ± 4.5%, respectively), without any significant difference. However, the amount of collagen synthetized (TCC) and the resulting TIR value were significantly ($p<0.01$) lower in the PCO-DG in comparison to healthy group implanted with the PCO scaffold (PCO-HG) (11.8 ± 1.6% vs. 19.0 ± 2.1% for TCC, and 29.2 ± 2.6% vs. 41.4 ± 3.8% for TIR, for PCO-DG and PCO-HG, respectively). When comparing the relative amount of ingrown cells with respect to the amount of collagen generated in percent, the diabetic group had the highest cell rate (147.4%) followed by the PCO-HG group (117.9%) and the DA50-HG group (74.6%).

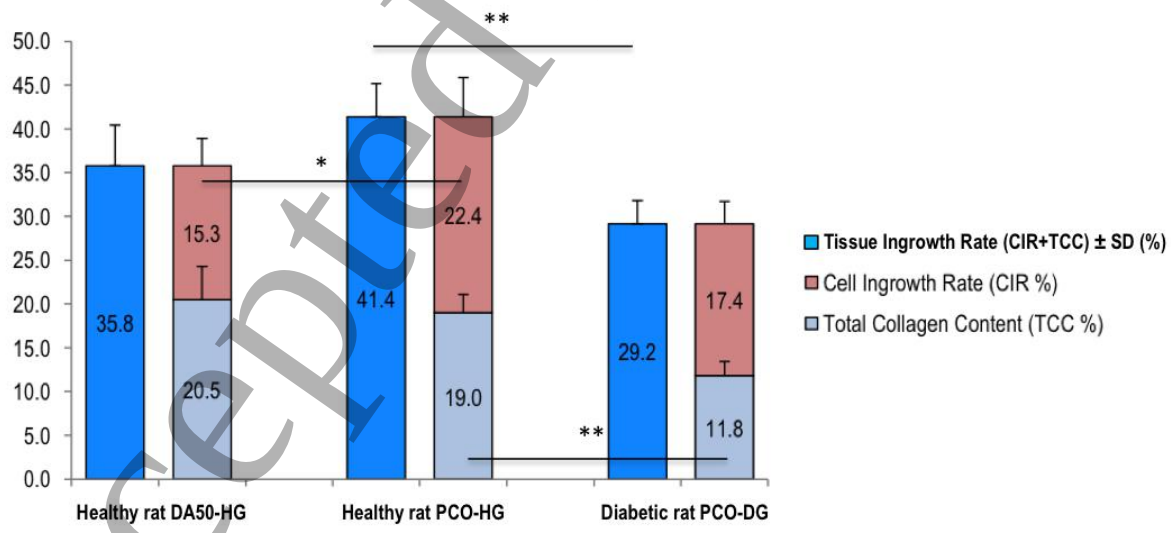

Figure 3. Tissue Ingrowth Rate (%) and sub-parameters at 21 days (n=5/group). *p<0.05 **p<0.001

Regarding the collagen polymorphism, although no statistical difference was noted among the groups, the ratio collagen I/collagen III was lower in the diabetic group (0.7 ± 0.3) compared to that in the PCO-HG group (1.2 ± 1.1) and higher in the DA50-HG (1.6 ± 1.1) vs. PCO-HG (table 2).

The collagen optical anisotropy value, reflecting the collagen maturity, was significantly lower in the diabetic animals (67.2 ± 10.8%) compared to that in the PCO-HG (79.3 ± 10.4%). In the DA50-HG (89.0 ± 22.7%), higher value of collagen anisotropy was obtained with respect to the PCO-HG group, without significant difference (anisotropy heterogeneity).

There was no significant difference in terms of collagen organization among animals in the three groups. Results of collagen directionality showed a predominant horizontal alignment of the collagen fibers in all three animal groups, after 21 days implantation (angle of the dominant collagen direction ranging from 2.0 ± 11.2° to 11.2 ± 12.9°). The amount of collagen fibers involved in that reorganization (>70%) did not significantly differ across the groups reflecting similar pattern of directional changes of the collagen fibers in all groups.

Table 2. Collagen indicators extracted from the PR-stained slides (polarized light) at 21 days (n=5/group).

	Healthy rats		**Diabetic Rats**
Parameters	**PCO - HG**	**DA 50 - HG**	**PCO - DG**
Collagen polymorphism [ratio coll I/III] Mean (SD)	1.2 (1.1)	1.6 (1.1)	0.7 (0.3)
Anisotropy [Collagen maturity][1] % (SD)	79.3 (10.4)	89.0 (22.7)	67.2 (10.8)*
Collagen fibers directionality			
Dominant direction angle - Degree (SD)	11.2 (12.9)	3.1 (14.2)	2.0 (11.2)
Dispersion - Mean (SD)	20.0 (7.2)	17.7 (3.3)	19.9 (6.1)
Amount of dominant direction - % (SD)	77.4 (0.1)	71.0 (0.1)	77.4 (0.1)

Collagen maturity is considered here as a metric, because it is a relative value calculated from two indicators (SAM=site anisotropy median and RAM=reference anisotropy median) (CM= SAM/RAM x 100) [32]. The normalized value brought by this metric, indicates the degree of collagen matrix restoration with respect to the native tissue. * Statistical difference ($p < 0.01$) compared to group PCO-HG.

Discussion

Numerous therapeutic products have been developed in the last decades to improve soft tissue healing or regeneration, even in conditions known for poor wound healing (e.g. type 1 diabetes mellitus, peripheral vascular disease, collagen diseases, tobacco use, irradiated tissues…), and minimize patient discomfort, healing length, chronic pain, infection and disability [33-35]. The last generation of therapeutic products (combined or not with a mixture of bioactive factors) or cell-seeded for surgical treatment, all were developed to improve wound healing with reduced complications. However, in the design phase of new products, there was a lack of routine advanced and validated tools of evaluation for comparing and ranking experimental products [11,12,17]. More evidence for the efficacy of current and future advanced wound therapies was required for their appropriate use [35]. This study was aimed at developing of a novel, simple and robust computerized quantitative method to evaluate tissue ingrowth metrics, and particularly, cell colonization, extracellular matrix generation, structure, morphology and maturity.

Stains

Automatic quantitative measurements were achieved thanks to specific and conventional selected stains. For the quantitative evaluation of the newly formed collagen, picrosirius red (PR) stain was preferred to Masson's Trichrom stain. Masson's Trichrome stain was generally associated with variations in staining intensity, hue, contrast and fading. Picrosirius red F3BA stain was a more selective and precise histochemical stain for collagen detection allowing even for collagen type identification under polarized light [28,36,37]. Moreover, in a study of cardiac allograft fibrosis, there was an excellent correlation between digital quantitative analysis of PR-stained collagen and the biochemical hydroxyproline (collagen) analysis [38]. In the present study, the total collagen content measurement was performed under standard bright field microscope of PR-stained sections because this method was validated in another study, where comparison to linear (cross) polarization quantification, revealed less collagen material in renal fibrosis analysis [39]. To quantify cellularity, the Feulgen & Rosenbeck stain was selected as a nuclear DNA stain. Use of this stain eliminates artifactual interferences that are observed with the traditional hematoxylin stain enabling the staining of other basophilic components of the tissues [29] or biomaterial basophilic components. Selection of those two stains enabled to set up a digital standard operating procedure with reduced operator corrections.

Cellularity

The analysis was performed 21 days post-implantation, where the major cellular players are encountered in the proliferative phase of the tissue healing around the scaffold yarns. In this proliferation phase, the preceding inflammatory cells and the newly arrived reconstructive cells participate actively in the healing process and is assumed to constitute a phase in which the specific contribution of a novel therapy may be identified. The reconstructive cells did not include only fibroblasts or fibrocytes, because it was recently shown that bone marrow (BM) derived mesenchymal cells play an important role in the wound healing. Using a mouse model, green fluorescent protein (GFP+) BM-derived cells accounted for 8.7% of total fibroblast-shaped cells in the normal skin. The proportion of GFP+ fibroblast-shaped BM-derived cells markedly increased (32.2 ± 4.8%) after wounding [40,41]. Myofibroblasts are a specialized form of fibroblast responsible for the deposition of a dense, fibrotic collagen matrix. They play a major role in wound contraction [42]. Hardly distinguishable morphologically, the fibroblasts, fibrocytes, myofibroblasts and mesenchymal cells were considered together as being the reconstructive cells for the histopathological analysis. The inflammatory and reconstructive cells were pooled for the quantitative analysis at this proliferation phase.

In this study, the chemically modified scaffold (DA50-HG) was associated with significantly fewer cells but with similar level of collagen production (TCC) compared to the non-modified scaffold (PCO-HG). Therefore, the chemically modified scaffold (DA50-HG) seems to induce a significant modulatory effect on the cellularity. As the inflammatory infiltrates profile were semi-quantitatively similar in those two healthy groups (DA50-HG and PCO-HG), it is presumed that the collagen production is ensured by a fewer reconstructive cells in the DA50-HG. By consequence, the chemically modified scaffold likely induced a modulation on both the cells and the collagen synthesis.

Relative to the collagen matrix laid down, our observations indicated a higher cellularity in diabetic rats in comparison to the other groups. These findings were consistent with the literature [25-27]. Given the low amount of collagen matrix produced in the diabetic group, it is assumed that the

cellularity was rather dominated by inflammatory cells than by reconstructive cells. It has been demonstrated than in delayed healing, the inflammatory cells in excess release significant amounts of enzymes such as collagenase (matrix metalloproteinase-8) destroying the connective tissue, or elastase able of eliminating critical growth factors such as PDGF and TGF-ß [43,44]. The computerized cellular analysis used in this study proved to be sensitive in demonstrating important CIR variation among the groups that could not be clearly evidenced with the semi-quantitative analysis.

Total collagen content

Collagen is the most abundant proteins of the extracellular matrix with a broad range of functions, including structural integrity, cell adhesion, cell migration, tissue morphogenesis, tissue scaffolding, and tissue repair (regulates the resident and inflammatory cell function) [42]. In a normal wound healing, the collagen matrix forms in a dynamics fashion with a constant remodeling. In pathologic response, fibrosis (excess of collagen) or altered collagen matrix (underproduction) may occur. Quantification of the amount of collagen generated may identify normal or pathological response to a given treatment. For example, it was demonstrated 7 times higher collagen in hypertrophic scar and 20 times higher collagen in keloidal scar than in normotrophic scar [42,45]. In this study, the total collagen content measured in the diabetic group (PCO-DG), may translate a significant slower collagen deposition compared to the healthy group (PCO-HG). These findings were in line with the published data [25-27], demonstrating that the computerized method used in this study enabled to quantify a pathological response with respect to the physiological response obtained in the group PCO-HG. In the healthy groups, no significant difference in collagen matrix production could be detected, what may be supportive of similar matrix functionality in the two healthy group (PCO-HG and DA50-HG). No excessive collagen matrix was formed.

Collagen polymorphism (collagen I and collagen III)

When tissue sections stained with picrosirius red stain are observed under a polarized light, it is possible to identify a few subtypes of collagen [28]. Collagen type I has a red-orange birefringence while collagen type III has a green birefringence, but it has been reported that picrosirius red-staining is unable to differentiate collagen subtypes [46,47]. The last author pointed out that the color of the collagen types depended on the orientation of the collagens. We observed those features as well in native unaffected dense collagen matrices (dermal tissue, muscular fascia, tendon, and ligament). Still, we were not able to confirm those findings in early formation of collagen matrix or in lymphoid organs. It has been demonstrated that in the early stages of wound healing, synthesis of collagen type III (thin and reticulated loose fibrils) are remodeled overtime with gradual increase of collagen type I (thicker and denser fibrils) deposition [42,48]. Recently, demonstrated a perfect correlation between PR-polarization procedure and Western blot analysis evaluating collagen type III and type I changes up to 180 days, in rabbit corneas [49]. Lymphoid organs are known to be composed of collagen type III in their parenchyma and of collagen type I in the fibrous capsule. We verified those biologic data in spleen and were subsequently able to use PR-stained rabbit spleen as a control tissue for collagen polymorphism investigation under polarized light [30].

In the present study, the ratio of collagen I/collagen III was 1.2 ± 1.1 for the PCO-HG group, 1.6 ± 1.1 for the DA50-HG group and 0.7 ± 0.3 for the diabetic group indicating a higher proportion of collagen type III relative to collagen type I in the diabetic group compared to the other two groups. The increased and sustained amounts of collagen III relative to collagen I indicates that tissues from animals in the diabetic group have immature collagen with retarded tissue healing [42]. These results

indicate that polarization of tissue stained with picrosirius red was adequate for the investigation of collagen type I and collagen type III over early healing time points. In native dense collagenous tissues, late stages of collagen remodeling, certain pathologic conditions, or artifactual interference (including improper preparation), caution should be taken in the interpretation of the collagen polymorphism [30,46]. The main reason is because the investigative PR-polarization procedure is not a phenotyping detection method but rather a biophysical means of determination based on topo-optical reaction of collagen subtypes.

Anisotropy properties of the collagen

Newly formed collagen undergoes maturation overtime [31,50-52]. The maturational process consists mainly of collagen remodeling by metallo-proteinases (MMPs) with shift of synthesis of collagen III to collagen I, intramolecular and intermolecular cross-linking, continuous loss of interstitial ground substance and water, increase in molecular fibrillar size and an organization which enhances mechanical properties. While those dynamic molecular changes are not obvious with use of bright field microscopy, use of the PR-polarization procedure identifies changes based on the optical anisotropy properties (birefringence) of the collagen that increases in brightness with the healing time [31]. The PR stain has the ability to noticeably amplify (7 times) the optical anisotropy properties of the collagen fibers (topo-optical reaction) thus increasing the usefulness of this stain in computational image analysis [28]. By using the rat fibrotic lesion model, Pickering and Boughner (1991) identified an accumulation of newly formed collagen that leveled off after 21 days[31]. However, the optical anisotropy of newly formed collagen progressively increased in intensity, through the entire length of their study (63 days), indicating that collagen changes beyond tissue repair. The results of the optical anisotropy time-course study were concordant with the results of a previous biomechanical study [53]. In this last study, the tensile strength values obtained from healing rat skin reached a maximum 90 days post-injury. The authors [31] concluded that using their method (quantification of fibrotic lesions using polarized light) helped to determine the age of a scar and to monitor changes in mechanical properties of generated tissues. In another study, using electron microscopy, an increase of the optical anisotropy intensity coincided with increase in the number of collagen fibrils with large diameter in old hearts [51].

In the present study, the intensity of the optical anisotropy was significantly lower in the diabetic group compared to the PCO-HG group. The low anisotropic value measured in the diabetic group might not reflect only higher value of collagen type III but molecular changes abnormalities of the newly formed collagen. Aldrovani *et al* (2007) reported that hyperglycemia noted with endocrine disorders causes nonenzymatic glycosylation of the collagen and other extracellular proteins [54]. These findings allow thinking that gauging the optical anisotropic properties of the collagen could be an indirect means to investigate the molecular effect of treatments on the extracellular response. Collectively, these quantitative findings indicate that animals in the diabetic group have regenerated tissue that is of poorer quality and mechanically weaker. Connizzo *et al* (2014) demonstrated that diabetes alters tendon mechanical properties and the dynamic response to load [55]. The group DA50-HG had a higher value of collagen anisotropy intensity, but no significant difference was established in comparison to the PCO-HG. A similar trend was observed with the ratio of collagen type I/collagen type III. The highest ratio value was obtained in the DA50-HG group without significance in comparison to the PCO-HG group. All these findings translate a trend for the collagen in the group DA50-HG to mature faster relative to the group PCO-HG. Knowing that the cellularity (CIR) was significantly lower in the DA50-HG group in comparison to the PCO-HG group,

compositional and structural modulation of the regenerated tissue seemed to be induced by the chemically modified scaffold in the DA50-HG group. The chemically modified collagen-chitosan film likely had an influence on the composition and structure of the generated tissue. These fine differences could not be observed at the semi-quantitative evaluation which may confirm the subjectivity and lack of discriminative power of the semi-quantitative analysis and emphasize the sensitivity of the computerized method devised in this study.

Collagen Directionality

The algorithm has been verified and validated against manual measurements of periodontal ligament direction (angle) in rats. The directionality measurements were more accurate with PR –polarization images than with bright field images (data not shown).

In this study, a similar pattern of directional changes of the collagen fibers was measured in all groups. The collagen fibers overhaul and realignment followed the peritoneal and abdominal wall plane. These findings suggested that the directional organization of the collagen was driven by the lines of mechanical tension as to withstand distension of the abdominal wall. The results indicated that the directional organization of the collagen fibers was irrespective of the animal health status or scaffold changes. Many authors demonstrated that orientation of the collagen fibers depended on the mechanical stress [56–58].

The mechanical quality of an ingrowing tissue did not depend only on the orientation of the collagen fibers but on other parameters such as the composition of the collagen subtypes (I and III) and structural organization. For instance, in saccular aneurysm, it was found that the wall strength was related to both collagen fiber strength and orientation [57]. It was demonstrated in patients that the ratio of collagen type I to collagen III was significantly lower for patients with hernia recurrence (1.3 ± 0.7) in comparison to those experiencing chronic pain (3.4 ± 1.2) or infection (2.9 ± 1.6) [59]. These results indicate the dependence of abdominal wall mechanical stability on collagen composition [58,60,61]. Therefore, the collagen density, collagen directionality, ratio of collagen I/collagen III and the optical anisotropy property of the collagen fibers should be considered together before qualifying the functionality of a regenerated tissue [62]. Obtaining those detailed and fine collagen data needs then a quantification approach as almost impossible to achieve qualitatively or semi-quantitatively without spending considerable amount of time.

Hypotheses validation

The validation of the proposed method was demonstrated by comparing the local effects and performance of scaffolds in healthy rats in comparison to diabetic rats, with expected significant differences in terms of cell ingrowth rate and new tissue formation rate [27,63]. A significant lower tissue ingrowth rate was observed with the diabetic rats (29.2 ± 2.6 %) versus healthy rats (41.4 ± 3.8 %). Noteworthy, in the present study, the most impaired factor caused by diabetes was new collagen formation. Cell ingrowth rate was less affected. These findings were concordant with the semi-quantitative histologic ratings, but were clearly evidenced (statistical significant differences) by the quantitative analysis.

It was also assumed that changes in chemical composition of the implants should impact the tissue ingrowth in a measurable way by quantitative histomorphometry, both in terms of cell colonization and new collagen formation. The cell colonization (CIR) was significantly lower in the chemical modified composite 3D scaffold group (DA50-HG) in comparison to the PCO-HG (15.3 ± 3.1 % versus 22.4 ± 4.5%, respectively). Although not significant, the tissue ingrowth rate was also lower for the

DA50-HG vs. PCO-HG (35.8 ± 4.7% vs. 41.4 ± 3.8%, respectively). These findings showed this quantitative method was more sensitive than the semi-quantitative approach, where no difference was noted between the two groups for cellularity or tissue ingrowth parameters.

The digital quantitative method developed in this study validated the two hypotheses stated in the introduction: 1) It was quantitatively demonstrated a significant delayed wound healing and poorer tissue in diabetics. 2) It was quantitatively demonstrated a significant tissue ingrowth modulation following chemical changes of the implant. The present digital method generated adds value to the conventional normative qualitative and semi-quantitative analyses particularly in terms of performance evaluation. Significant differences were established from the computational quantitative analysis in terms of i) cellularity (CIR) showing DA50-HG < PCO-HG, ii) collagen produced (TCC) showing PCO-DG < PCO-HG and finally iii) tissue ingrowth (TIR) pointing out PCO-DG < PCO-HG, that were not detected at the semi-quantitative analysis. The cellularity evaluated semi-quantitatively (table 1) was similar for groups PCO-HG and DA50-HG, but greater than in the PCO-DG. Fine histomorphometric differences ranged within 8-10% indicating statistical significance could not be detected semi-quantitatively. The other quantitative indicators (ratio collagen I/III, collagen maturity, collagen directionality) could not be directly correlated with semi-quantitative analysis as they could not be evaluated semi-quantitatively.

The automated method is validated for evaluation of the following parameters (CIR corresponding to the cellularity parameters in the semi-quantitative analysis; TCC corresponding to the sum of fibroplasia and fibrosis; TIR corresponding to the tissue ingrowth). So far, semi-quantitative analysis remains necessary to assess the different cell population associated with the regenerated tissue to better qualify the inflammation and foreign body reaction elicited by soft tissue therapeutic products. The simple and supervised automated method used in this study to assess the performance of intraperitoneal mesh can be broadened to the evaluation of any porous scaffolds used for soft tissue repair or in regenerative surgeries (e.g. urinary tract reconstruction, dermal wound healing, ligament reconstruction, periodontal regeneration, hernia repair [64] or in the evaluation of fibrotic disorders [65]. Further studies are needed to assess the sensitivity and specificity of the present method.

Conclusion

The innovative computerized method devised in this study allowed fine and detailed objective evaluation of the soft tissues growth. This new method refered to by the authors as SCAN-CT (structural and compositional computerized analysis of connective tissue) could be applied in routine to measure the added value of a new functional regenerative strategy. It provides key metrics for structural and compositional characterization of repaired or regenerated tissues and is sensitive in the determination of the cell ingrowth rate, total collagen content, tissue ingrowth rate, collagen polymorphism, directional organization of the collagen and the optical anisotropy properties of the collagen. In routine biomaterials pathology, detailed extracellular response is often overlooked compared to cellular response, while collagen matrix is a reservoir of insightful information. By digitally exploiting the picrosirius-polarization procedure a bunch of complementary quantitative data on the collagen polymorphism (collagen I and collagen III), the directional organization of the collagen and the optical anisotropy properties of the collagen (maturation) could be extracted from the same slide. This computer assisted image analysis approach allowed for elucidating the quality, matrix restoration, integrity, composition and function of the regenerated tissue. Furthermore, it

proved to be simple, sensitive, and economically affordable than series of immunohistochemical, molecular or biochemical methods. Compared to other methods, such as immunohistochemistry, the present method has the advantage of preserving in situ morphological features of the treated tissues for their descriptive investigation and histological proof. Both hypotheses defined in this study were validated and permitted to consider this digital quantitative pathology tool as suitable for routine and concise characterization of soft tissue healing performance in an objective way with reduced examiner dependency.

Acknowledgements

The authors gratefully acknowledge Dr Elodie Devron Gaillot, Pathologist, for reviewing the slides as independent reader, Dr James Render, Pathologist, to have carefully reviewed the manuscript, and Paul Bonijol, Engineer, for his contribution in the adaptation of part of the algorithms of this project. Funding for this research was partly supported by the Fonds Unique Interministériel (FUI) program (No AAP:15—Project No F1312025 V REVAMED – Régénération et Evaluation des Dispositifs Médicaux). No competing financial interests exist.

Conflict of interest

The authors declare that there is no conflict of interest, financial or otherwise regarding the publication of this paper.

References

[1] W.R. Sewell, J. Wiland, B.N. Craver, A new method of comparing sutures of ovine catgut with sutures of bovine catgut in three species, Surg. Gynecol. Obstet. 100 (1955) 483–494.

[2] E.J. van Rijssel, J.B. Trimbos, A. da Costa, G.J. Fleuren, R. Brand, Assessment of tissue reaction at suture knots; an adaptation of Sewell's scoring system, Eur. J. Obstet. Gynecol. Reprod. Biol. 27 (1988) 165– 172.

[3] 10993-6 ISO, International Organization for Standardization (ISO) 10993-6, Biological evaluation of medical devices - Part 6: Tests for local effects after implantation, (2016).

[4] T.G. van Tienen, R.G.J.C. Heijkants, P. Buma, J.H. de Groot, A.J. Pennings, R.P.H. Veth, Tissue ingrowth and degradation of two biodegradable porous polymers with different porosities and pore sizes, Biomaterials. 23 (2002) 1731–1738.

[5] M.D. Markel, M.A. Wikenheiser, R.L. Morin, D.G. Lewallen, E.Y. Chao, Quantification of bone healing. Comparison of QCT, SPA, MRI, and DEXA in dog osteotomies, Acta Orthop. Scand. 61 (1990) 487–498.

[6] E. Lespessailles, C. Chappard, N. Bonnet, C.L. Benhamou, Imaging techniques for evaluating bone microarchitecture, Jt. Bone Spine Rev. Rhum. 73 (2006) 254–261. doi:10.1016/j.jbspin.2005.12.002.

[7] J.H.D. Bassett, A. van der Spek, A. Gogakos, G.R. Williams, Quantitative X-ray imaging of rodent bone by Faxitron, Methods Mol. Biol. Clifton NJ. 816 (2012) 499–506. doi:10.1007/978-1-61779-415-5_29.

[8] D.J. Saliken, T.D. Bornes, M.J. Bouliane, D.M. Sheps, L.A. Beaupre, Imaging methods for quantifying glenoid and Hill-Sachs bone loss in traumatic instability of the shoulder: a scoping review, BMC Musculoskelet. Disord. 16 (2015) 164. doi:10.1186/s12891-015-0607-1.

[9] D.W. Dempster, J.E. Compston, M.K. Drezner, F.H. Glorieux, J.A. Kanis, H. Malluche, P.J. Meunier, S.M. Ott, R.R. Recker, A.M. Parfitt, Standardized nomenclature, symbols, and units for bone histomorphometry: a 2012 update of the report of the ASBMR Histomorphometry Nomenclature

Committee, J. Bone Miner. Res. Off. J. Am. Soc. Bone Miner. Res. 28 (2013) 2–17. doi:10.1002/jbmr.1805.

[10] K. Gritsch, N. Laroche, L. Morgon, R. Al-Hity, L. Vico, P. Colon, B. Grosgogeat, A systematic review of methods for tissue analysis in animal studies on orthodontic mini-implants, Orthod. Craniofac. Res. 15 (2012) 135–147. doi:10.1111/j.1601-6343.2012.01548.x.

[11] A. Gupta, P. Kumar, Assessment of the histological state of the healing wound, Plast. Aesthetic Res. 2 (2015) 239. doi:10.4103/2347-9264.158862.

[12] R.E. Guldberg, C.L. Duvall, A. Peister, M.E. Oest, A.S.P. Lin, A.W. Palmer, M.E. Levenston, 3D imaging of tissue integration with porous biomaterials, Biomaterials. 29 (2008) 3757–3761. doi:10.1016/j.biomaterials.2008.06.018.

[13] C.J. Kirkpatrick, V. Krump-Konvalinkova, R.E. Unger, F. Bittinger, M. Otto, K. Peters, Tissue response and biomaterial integration: the efficacy of in vitro methods, Biomol. Eng. 19 (2002) 211–217.

[14] M.P. Lutolf, F.E. Weber, H.G. Schmoekel, J.C. Schense, T. Kohler, R. Müller, J.A. Hubbell, Repair of bone defects using synthetic mimetics of collagenous extracellular matrices, Nat. Biotechnol. 21 (2003) 513–518. doi:10.1038/nbt818.

[15] M. Ventre, F. Causa, P.A. Netti, Determinants of cell-material crosstalk at the interface: towards engineering of cell instructive materials, J. R. Soc. Interface. 9 (2012) 2017–2032. doi:10.1098/rsif.2012.0308.

[16] F. Colombo, G. Sampogna, G. Cocozza, S.Y. Guraya, A. Forgione, Regenerative medicine: clinical applications and future perspectives, Journal of Microscopy and Ultrastructure, 5 (2017) 1-8. https://doi.org/10.1016/j.jmau.2016.05.002.

[17] N.N. Ramrattan, R.G.J.C. Heijkants, T.G. van Tienen, A.J. Schouten, R.P.H. Veth, P. Buma, Assessment of tissue ingrowth rates in polyurethane scaffolds for tissue engineering, Tissue Eng. 11 (2005) 1212–1223. doi:10.1089/ten.2005.11.1212.

[18] M.C. Wake, A.G. Mikos, G. Sarakinos, J.P. Vacanti, R. Langer, Dynamics of fibrovascular tissue ingrowth in hydrogel foams, Cell Transplant. 4 (1995) 275–279.

[19] M.P. Chhaya, E.R. Balmayor, D.W. Hutmacher, J.T. Schantz. Transformation of breast reconstruction via additive biomanufacturing. Sci Rep. 6 (2016) 1-12. doi: 10.1038/srep28030.

[20] M.T. Wolf, C.A. Carruthers, C.L. Dearth, P.M. Crapo, A. Huber, O.A. Burnsed, R. Londono, S.A. Johnson, K.A. Daly, E.C. Stahl, J.M. Freund, C.J. Medberry, L.E. Carey, A. Nieponice, N.J. Amoroso, S.F. Badylak. Polypropylene Surgical Mesh Coated with Extracellular Matrix Mitigates the Host Foreign Body Response. Biomed Mater Res A. 102 (2014) 234–246. doi:10.1002/jbm.a.34671.

[21] T. Yamamoto, M. Wakita, The development and structure of principal fibers and cellular cementum in rat molars, J. Periodontal Res. 26 (1991) 129–137.

[22] R.B. Diller, R.G. Audet, R.S. Kellar, Quantitative Histopathology for Evaluation of In Vivo Biocompatibility Associated with Biomedical Implants, in: S.J. Potts, D.A. Eberhard, K.A. Wharton, (Eds.), Mol. Histopathol. Tissue Biomark. Drug Diagn. Dev., Springer New York, New York, NY, 2014: pp. 153–162. doi:10.1007/7653_2014_37.

[23] H.S. Baik, J. Park, K.J. Lee, C. Chung, Local application of periodontal ligament stromal cells promotes soft tissue regeneration, Oral Dis. 20 (2014) 574-581. doi: 10.1111/odi.12175.

[24] D. Ulrich, I. Le Teuff, S. Huberlant, P. Carteron, V. Letouzey, R. de Tayrac, A preclinical evaluation of polypropylene/polylacticacid hybrid meshes for fascial defect repair using a rat abdominal hernia model, PLoS One 12 (2017) doi: 10.1371/journal.pone.0179246.

[25] S. Mclennan, D. Yue, S. Twigg, Molecular aspects of wound healing in diabetes, 14 (2006) 8–13.

[26] H. Brem, M. Tomic-Canic, Cellular and molecular basis of wound healing in diabetes, J. Clin. Invest. 117 (2007) 1219–1222. doi:10.1172/JCI32169.

[27] E. Tsourdi, A. Barthel, H. Rietzsch, A. Reichel, S.R. Bornstein, Current aspects in the pathophysiology and treatment of chronic wounds in diabetes mellitus, BioMed Res. Int. 2013 (2013) 385641. doi:10.1155/2013/385641.

[28] L.C. Junqueira, W. Cossermelli, R. Brentani, Differential staining of collagens type I, II and III by Sirius Red and polarization microscopy, Arch. Histol. Jpn. Nihon Soshikigaku Kiroku. 41 (1978) 267–274.

[29] J.M. Exbrayat, Genome visualization by classic methods in light microscopy, CRC Press, 2001.

[30] A. Alves, K. Gritsch, C. Sirieix, E. Drevon-Gaillot, Y. Bayon, G. Clermont, J.-P. Boutrand, B. Grosgogeat, Computerized histomorphometric study of the splenic collagen polymorphism: A control-tissue for polarization microscopy: Histomorphometric Study of the Splenic Collagen, Microsc. Res. Tech. 78 (2015) 900–907. doi:10.1002/jemt.22553.

[31] J.G. Pickering, D.R. Boughner, Quantitative assessment of the age of fibrotic lesions using polarized light microscopy and digital image analysis, Am. J. Pathol. 138 (1991) 1225–1231.

[32] D. Bours, On indicators, measures and metrics. A recap, (2014). https://www.linkedin.com/pulse/20141002153744-18927814-on-indicators-measures-and-metrics-recap.

[33] M.D. Menger, P. Walter, F. Hammersen, K. Messmer, Quantitative analysis of neovascularization of different PTFE-implants, Eur. J. Cardio-Thorac. Surg. Off. J. Eur. Assoc. Cardio-Thorac. Surg. 4 (1990) 191–196.

[34] A.P. Sclafani, R. Thomas, J.L. McCormick, V.K. Sherwin, J. May S Jacobson, Modulation of Wound Response and Soft Tissue Ingrowth in Synthetic and Allogeneic Implants With Platelet Concentrate, Arch Facial Plast Surg. 3 (2005) 163–169.

[35] R.G. Frykberg, J. Banks, Challenges in the Treatment of Chronic Wounds, Adv. Wound Care. 4 (2015) 560–582. doi:10.1089/wound.2015.0635.

[36] Y. Huang, W.B. de Boer, L.A. Adams, G. MacQuillan, E. Rossi, P. Rigby, S.C. Raftopoulos, M. Bulsara, G.P. Jeffrey, Image analysis of liver collagen using sirius red is more accurate and correlates better with serum fibrosis markers than trichrome, Liver Int. 33 (2013) 1249–1256. doi:10.1111/liv.12184.

[37] Z. Kmiec, J.A. Kiernan. Histological and Histochemical Methods: Theory and Practice. 5th edition, Scion Publishing, 2015, 571 pp, Folia Histochem. Cytobiol. 54 (2016) 58–59. doi:10.5603/FHC.a2016.0007.

[38] J.G. Pickering, D.R. Boughner, Fibrosis in the transplanted heart and its relation to donor ischemic time. Assessment with polarized light microscopy and digital image analysis, Circulation. 81 (1990) 949–958.

[39] M.M. Diaz Encarnacion, M.D. Griffin, J.M. Slezak, E.J. Bergstralh, M.D. Stegall, J.A. Velosa, J.P. Grande, Correlation of Quantitative Digital Image Analysis with the Glomerular Filtration Rate in Chronic Allograft Nephropathy: Digital Image Analysis in Chronic Rejection, Am. J. Transplant. 4 (2004) 248– 256. doi:10.1046/j.1600-6143.2003.00311.x.

[40] G. Ishii, T. Sangai, K. Sugiyama, T. Ito, T. Hasebe, Y. Endoh, J. Magae, A. Ochiai, In vivo characterization of bone marrow-derived fibroblasts recruited into fibrotic lesions, Stem Cells Dayt. Ohio. 23 (2005) 699–706. doi:10.1634/stemcells.2004-0183.

[41] Y. Wu, J. Wang, P.G. Scott, E.E. Tredget, Bone marrow-derived stem cells in wound healing: a review, Wound Repair Regen. Off. Publ. Wound Heal. Soc. Eur. Tissue Repair Soc. 15 Suppl 1 (2007) S18-26. doi:10.1111/j.1524-475X.2007.00221.x.

[42] M. Xue, C.J. Jackson, Extracellular Matrix Reorganization During Wound Healing and Its Impact on Abnormal Scarring, Adv. Wound Care. 4 (2015) 119–136. doi:10.1089/wound.2013.0485.

[43] B.C. Nwomeh, H.X. Liang, I.K. Cohen, D.R. Yager, MMP-8 is the predominant collagenase in healing wounds and nonhealing ulcers, J. Surg. Res. 81 (1999) 189–195. doi:10.1006/jsre.1998.5495.

[44] R.F. Diegelmann, M.C. Evans, Wound healing: an overview of acute, fibrotic and delayed healing, Front. Biosci. J. Virtual Libr. 9 (2004) 283–289.

[45] P.D.H.M. Verhaegen, P.P.M. van Zuijlen, N.M. Pennings, J. van Marle, F.B. Niessen, C.M.A.M. van der Horst, E. Middelkoop, Differences in collagen architecture between keloid, hypertrophic scar, normotrophic scar, and normal skin: An objective histopathological analysis, Wound Repair Regen. Off. Publ. Wound Heal. Soc. Eur. Tissue Repair Soc. 17 (2009) 649–656. doi:10.1111/j.1524-475X.2009.00533.x.

[46] L.C. Junqueira, G.S. Montes, E.M. Sanchez, The influence of tissue section thickness on the study of collagen by the Picrosirius-polarization method, Histochemistry. 74 (1982) 153–156.

[47] L. Rich, P. Whittaker, COLLAGEN AND PICROSIRIUS RED STAINING: A POLARIZED LIGHT ASSESSMENT OF FIBRILLAR HUE AND SPATIAL DISTRIBUTION, Braz. J. morphol. Sci. 22 (2005) 97–104.

[48] J.N. Clore, I.K. Cohen, R.F. Diegelmann, Quantitation of collagen types I and III during wound healing in rat skin, Proc. Soc. Exp. Biol. Med. Soc. Exp. Biol. Med. N. Y. N. 161 (1979) 337–340.

[49] Y. Xia, B. Liu, Z. Fan, X. Peng, Corneal Collagen Fibril Changes After Ultraviolet A/Riboflavin Corneal Crosslinking:, Cornea. 33 (2014) 56–59. doi:10.1097/ICO.0000000000000017.

[50] H.G. Vogel, Influence of maturation and aging on mechanical and biochemical properties of connective tissue in rats, Mech. Ageing Dev. 14 (1980) 283–292.

[51] C.R. Gazoti Debessa, L.B. Mesiano Maifrino, R. Rodrigues de Souza, Age related changes of the collagen network of the human heart, Mech. Ageing Dev. 122 (2001) 1049–1058.

[52] C.C. Yates, P. Hebda, A. Wells, Skin wound healing and scarring: fetal wounds and regenerative restitution, Birth Defects Res. Part C Embryo Today Rev. 96 (2012) 325–333. doi:10.1002/bdrc.21024.

[53] S.M. Levenson, E.F. Geever, L.V. Crowley, J.F. Oates, C.W. Berard, H. Rosen, The healing of rat skin wounds, Ann. Surg. 161 (1965) 293–308.

[54] M. Aldrovani, A.M.A. Guaraldo, B.C. Vidal, Optical anisotropies in corneal stroma collagen fibers from diabetic spontaneous mice, Vision Res. 47 (2007) 3229–3237. doi:10.1016/j.visres.2007.02.011.

[55] B.K. Connizzo, P.R. Bhatt, K.W. Liechty, L.J. Soslowsky, Diabetes alters mechanical properties and collagen fiber re-alignment in multiple mouse tendons, Ann. Biomed. Eng. 42 (2014) 1880–1888. doi:10.1007/s10439-014-1031-7.

[56] K. Suda, K. Abe, K. Kaneda, Changes in the orientation of collagen fibers on the superficial layer of the mouse tibial bone after denervation: scanning electron microscopic observations, Arch. Histol. Cytol. 62 (1999) 231–235.

[57] D.J. MacDonald, H.M. Finlay, P.B. Canham, Directional wall strength in saccular brain aneurysms from polarized light microscopy, Ann. Biomed. Eng. 28 (2000) 533–542.

[58] H. Hjort, T. Mathisen, A. Alves, G. Clermont, J.P. Boutrand, Three-year results from a preclinical implantation study of a long-term resorbable surgical mesh with time-dependent mechanical characteristics, Hernia J. Hernias Abdom. Wall Surg. 16 (2012) 191–197. doi:10.1007/s10029-011-0885-y.

[59] K. Junge, U. Klinge, R. Rosch, P. Lynen, M. Binnebösel, J. Conze, P.R. Mertens, R. Schwab, V. Schumpelick, Improved collagen type I/III ratio at the interface of gentamicin-supplemented polyvinylidenfluoride mesh materials, Langenbecks Arch. Surg. 392 (2007) 465–471. doi:10.1007/s00423-006-0138-1.

[60] K. Junge, U. Klinge, R. Rosch, P.R. Mertens, J. Kirch, B. Klosterhalfen, P. Lynen, V. Schumpelick, Decreased collagen type I/III ratio in patients with recurring hernia after implantation of alloplastic prostheses, Langenbecks Arch. Surg. 389 (2004) 17–22. doi:10.1007/s00423-003-0429-8.

[61] S. Kalaba, E. Gerhard, J.S. Winder, E.M. Pauli, R.S. Haluck, J. Yang, Design Strategies and Applications of Biomaterials and Devices for Hernia Repair, Bioact. Mater. 1 (2016) 2–17. doi:10.1016/j.bioactmat.2016.05.002.

[62] K. Novak, S. Polzer, M. Tichy, J. Bursa, Automatic Evaluation of Collagen Fiber Directions from Polarized Light Microscopy Images, Microsc. Microanal. Off. J. Microsc. Soc. Am. Microbeam Anal. Soc. Microsc. Soc. Can. 21 (2015) 863–875. doi:10.1017/S1431927615000586.

[63] S. Guo, L.A. Dipietro, Factors affecting wound healing, J. Dent. Res. 89 (2010) 219–229. doi:10.1177/0022034509359125.

[64] R.L. Horan, D.S. Bramono, J.R.L. Stanley, Q. Simmons, J. Chen, H.E. Boepple, G.H. Altman, Biological and biomechanical assessment of a long-term bioresorbable silk-derived surgical mesh in an abdominal body wall defect model, Hernia J. Hernias Abdom. Wall Surg. 13 (2009) 189–199. doi:10.1007/s10029-008-0459-9.

[65] T.J. Koh, L.A. DiPietro, Inflammation and wound healing: the role of the macrophage, Expert Rev. Mol. Med. 13 (2011) e23. doi:10.1017/S1462399411001943.